Applied and Computational Mathematics
2025, Vol. 14, No. 4, pp. 223-240
https://doi.org/10.11648/j.acm.20251404.15

Research Article

Pulmonary Tuberculosis and Pneumonia Co-Dynamics: A Mathematical Modelling Approach

Erick Mutwiri Kirimi[1,*], Jeconiah Okelo[2], Mark Kimathi[3], Kenneth Ngure[4]

[1]Department of Mathematics, Pan African University Institute for Basic Sciences, Technology, and Innovation, Nairobi, Kenya

[2]Department of Pure and Applied Mathematics, Jomo Kenyatta University of Agriculture and Technology, Nairobi, Kenya

[3]Department of Mathematics and Statistics, Machakos University, Machakos, Kenya

[4]Department of Public and Community Health, Jomo Kenyatta University of Agriculture and Technology, Nairobi, Kenya

Abstract

This study presents a novel mathematical model that captures the co-dynamics of pulmonary tuberculosis in the presence of opportunistic pneumonia. The model integrates opportunistic pneumonia into the classical pulmonary tuberculosis transmission framework, based on clinical evidence of a lethal synergism between the two diseases. A Holling-type saturation function is utilized to reflect the impact of natural immunity on the progression from latent tuberculosis infection to active disease. Asymptomatic infectious individuals can transmit the infection unnoticed, thereby significantly contributing to the high rate of transmission. Thus, the screening of asymptomatic individuals is incorporated into the model as a strategy to mitigate the prevalence of co-infections. A comprehensive sensitivity analysis and numerical simulations were conducted to evaluate the effects of various interventions, including enhancing natural immunity, screening asymptomatic and latently infected individuals, improving vaccine efficacy, and treating patients with severe pulmonary tuberculosis. The sensitivity analysis reveals that improving vaccine efficacy is the most effective strategy for minimizing co-infections. Simulations also demonstrate that increased screening and treatment rates significantly reduce the burden of pulmonary tuberculosis-pneumonia co-infections. These results underscore the need to develop vaccines with higher efficacy to reduce co-infections of pulmonary tuberculosis and opportunistic pneumonia. Additionally, the study recommends expanded screening of asymptomatic tuberculosis cases and the strengthening of immunity among latently infected populations.

Keywords

Pulmonary Tuberculosis, Asymptomatic Infectious, Opportunistic Pneumonia, Latently Infected, Natural Immunity, Numerical Simulation

*Corresponding author: ercmutwiri@gmail.com (Erick Mutwiri Kirimi)

Received: 7 July 2025; **Accepted:** 22 July 2025; **Published:** 20 August 2025

1. Introduction

Pulmonary tuberculosis (TB) remains one of the leading infectious causes of mortality worldwide, particularly in low- and middle-income countries [1]. For instance, in Kenya alone, approximately 23,149 people succumbed to the disease in 2023 [2]. Despite significant progress in pulmonary tuberculosis control, challenges persist due to the complex interactions between pulmonary tuberculosis and other infections. One such infection is pneumonia, which often emerges as an opportunistic co-infection, especially in immunocompromised individuals suffering from active pulmonary tuberculosis [3]. Opportunistic pneumonia refers to lower respiratory tract infections that exploit weakened host immunity, a common consequence of chronic pulmonary tuberculosis infection. The coexistence of these diseases can exacerbate disease severity, complicate diagnosis and treatment, and increase the risk of transmission within affected communities [4]. Mathematical modeling of the co-dynamics of these diseases is therefore essential for designing effective intervention strategies that can prevent or mitigate their coexistence.

Mathematical modeling is a valuable tool for exploring the transmission dynamics of infectious diseases. It is widely used to predict the potential impact of interventions, as well as the interactions between multiple interventions during epidemics, while effectively capturing non-linear transmission dynamics [5]. In this study, a classical SEIR (Susceptible, Exposed, Infectious, Recovered) transmission framework is employed to formulate a novel mathematical model for the co-dynamics of pulmonary tuberculosis and opportunistic pneumonia. The objective is to accurately represent the natural progression of the co-infection and to suggest effective strategies for controlling its spread. The SEIR model, a widely used compartmental framework in mathematical epidemiology, describes the spread of infectious diseases that include a latent or exposed phase [6]. Epidemiological models of pulmonary tuberculosis often adopt the classical SEIR structure because approximately one-quarter of the global population harbors latent tuberculosis infections [7]. During the latent phase, individuals are neither infectious nor symptomatic; however, if left untreated, they may progress to pulmonary tuberculosis disease. Preventing the progression of latent tuberculosis infections to disease reduces the risk of further transmission within the population [8]. Therefore, this study predicts the effects of screening latently infected individuals on the co-existence of pulmonary tuberculosis and opportunistic pneumonia using a mathematical modeling approach.

Numerous mathematical models have been formulated to study pulmonary tuberculosis and pneumonia as independent diseases, with a focus on strategies to control the transmission of infections. In particular, models of pulmonary tuberculosis have contributed significantly to understanding its transmission dynamics and informing effective control measures [9-13]. For example, Wang et al. [14] formulated a mathematical model of pulmonary tuberculosis that incorporates age and spatial structures, treatment, and relapse. Their results suggest that reducing the transmission coefficient, decreasing the infectiousness of treated individuals, and increasing the treatment rate are feasible measures to control the transmission of pulmonary tuberculosis. Oshinubi et al. [15] formulated a mathematical model to assess the impact of vaccination and treatment strategies on pulmonary tuberculosis outbreaks in East Africa. The findings of their study indicated that increasing vaccination coverage and improving treatment strategies reduce the prevalence and burden of pulmonary tuberculosis in the human population. A hybrid mathematical model of pulmonary tuberculosis, combining equation-based and agent-based approaches and emphasizing the impact of human mobility on disease spread, was presented by [16]. The results of the study showed that human mobility significantly influences the spread of pulmonary tuberculosis within the population. Ochieng [17] formulated a novel mathematical model of tuberculosis incorporating reinfection, emphasizing the need for robust public health interventions. The findings of the study indicated that a 20% decrease in the transmission rate, coupled with a 5% increase in vaccine efficacy, would reduce tuberculosis transmission by 32.6% in Kenya.

Recent mathematical models have been developed to explore various aspects of pneumonia and to contribute to its containment. For example, Njeri et al. [18] formulated a mathematical model of pneumonia to assess the impact of misdiagnoses and vaccine efficacy. Their simulation results revealed that an increase in misdiagnoses led to greater disease persistence, while increased vaccination reduced infection transmission in the population. A mathematical model to assess the impact of pneumonia transmission dynamics in high-risk populations was formulated and analyzed by [19]. The study employed Latin hypercube sampling for global sensitivity analysis. Numerical results showed that prompt and effective treatment at the onset of the disease is essential to control the spread of pneumonia among children under five and adults over 65 years of age. Ndendya et al. [20] formulated a mathematical model of pneumonia to determine the impact of malnutrition on disease dynamics. Their deterministic model divided the population into two groups: well-nourished and undernourished, and sensitivity analysis was performed using the normalized forward sensitivity index. The results of their study show that individuals who are malnourished have a higher chance of acquiring and dying from pneumonia than well-nourished individuals. Other mathematical models of pneumonia, developed as essential tools for public health planning and the design of interventions, particularly in high-risk regions relevant to this study, include [21-26].

The novelty of the formulated model is presented in this section. Previous mathematical models describing the trans-

mission of pulmonary tuberculosis and pneumonia have not incorporated several key aspects addressed in the current study. First, many existing models assume that the progression rate from latent infection to pulmonary tuberculosis disease is directly proportional to the number of latently infected individuals. However, in reality, this progression is influenced by an individual's natural immunity [8]. This study rigorously predicts, through mathematical modeling, the impact of natural immunity on the reactivation of latent infections and its role in controlling or reducing the co-existence of pulmonary tuberculosis and opportunistic pneumonia. Second, the current model incorporates an asymptomatic infectious population, as these individuals continuously transmit the disease to susceptible individuals without detection, thereby significantly contributing to overall transmission. The inclusion of this compartment is justified by the 2025 WHO report, which revealed that approximately 50% of individuals with pulmonary tuberculosis identified through global prevalence surveys are asymptomatic yet infectious [27]. These findings suggest that targeting only symptomatic individuals is insufficient to halt transmission, as the disease will continue to spread through undetected asymptomatic carriers. In this study, numerical simulations are employed to predict the impact of screening and treating asymptomatic infectious individuals on controlling the co-existence of pulmonary tuberculosis and opportunistic pneumonia. Third, the model integrates opportunistic pneumonia into the mathematical framework for pulmonary tuberculosis, as clinical studies have shown a lethal synergism between the two diseases. Specifically, individuals infected with tuberculosis provide a conducive environment for aggressive pneumonia due to compromised immunity [28]. Therefore, the model leverages the synergies among prevention, screening, and treatment of both pulmonary tuberculosis and opportunistic pneumonia to inform strategies aimed at reducing their co-existence. The main objective of this research is to determine effective strategies for reducing the co-existence of pulmonary tuberculosis and opportunistic pneumonia. Consequently, the morbidity and mortality associated with this co-infection can be significantly reduced. Based on an extensive literature review, no previous study has addressed the specific research gaps identified in the present work.

The paper is organized as follows: Section 2 presents the model formulation, while Section 3 provides the mathematical analysis. Section 4 presents numerical simulations of the model to illustrate the impact of various intervention strategies on controlling the prevalence of pulmonary tuberculosis and opportunistic pneumonia co-infections. Finally, Section 5 concludes the study.

2. Model Formulation

The model partitions the total human population at time t, denoted by $N(t)$, into twelve compartments based on their epidemiological status. The model variables used in the formulation are $S(t)$, $V(t)$, $E(t)$, $I_a(t)$, $I_S(t)$, $I_{aP}(t)$, $I_{SP}(t)$, $T_a(t)$, $T_S(t)$, $T_{aP}(t)$, $T_{SP}(t)$, and $R(t)$, as defined in Table 1.

Table 1. *Definition of the model variables.*

Variable	Definition
$S(t)$	Individuals susceptible to pulmonary tuberculosis
$V(t)$	Individuals vaccinated against pulmonary tuberculosis
$E(t)$	Individuals latently infected with pulmonary tuberculosis
$I_a(t)$	Individuals with asymptomatic pulmonary tuberculosis
$I_S(t)$	Individuals with symptomatic pulmonary tuberculosis
$I_{aP}(t)$	Individuals with asymptomatic tuberculosis and pneumonia co-infection
$I_{SP}(t)$	Individuals with symptomatic tuberculosis and pneumonia co-infection
$T_a(t)$	Individuals with asymptomatic tuberculosis undergoing treatment
$T_S(t)$	Individuals with symptomatic tuberculosis undergoing treatment
$T_{aP}(t)$	Individuals with asymptomatic tuberculosis and pneumonia undergoing treatment
$T_{SP}(t)$	Individuals with symptomatic tuberculosis and pneumonia undergoing treatment
$R(t)$	Individuals who have recovered

Thus,

$$N(t) = S(t) + V(t) + E(t) + I_a(t) + I_S(t) + I_{aP}(t) + I_{SP}(t) + T_a(t) + T_S(t) + T_{aP}(t) + T_{SP}(t) + R(t)$$

The model introduced in this study incorporates a saturated progression rate from latent infection to active disease, accounting for natural immunity through Holling's-type saturation function, $\frac{\varepsilon E(t)}{1+nE(t)}$, as described in [29]. The number of latently infected individuals effectively saturates when immunity levels are high. In this function, ε represents the reactivation rate of latent infections, n quantifies the delay in reactivation due to enhanced immunity. When n approaches zero, corresponding to cases of extremely low immunity, the function approximates $\varepsilon E(t)$.

The formulation of the model involves transitions between compartments, representing changes from one disease state to another, and utilizes the parameters described in Table 2.

Table 2. *Description of the model parameters.*

Parameter	Description
Λ	Recruitment rate of individuals into the population.
Q	Proportion of individuals vaccinated.
ρ	Efficacy of the pulmonary tuberculosis vaccine.
$\lambda_1,\ \lambda_2$	Forces of infection for pulmonary tuberculosis and pneumonia, respectively.
μ	Natural death rate.
$\alpha_1,\ \vartheta_1,\ \vartheta_3,\ \vartheta_4$	Rates at which individuals with latent infection, asymptomatic TB, asymptomatic TB-pneumonia co-infection, and symptomatic TB-pneumonia co-infection are screened, respectively.
ϑ_2	Treatment rate of individuals with symptomatic tuberculosis.
$\varepsilon_1,\ \varepsilon_2$	Rates at which latently infected individuals progress to symptomatic TB and asymptomatic TB, respectively.
$\phi_1,\ \phi_2$	Rates at which individuals with asymptomatic TB and asymptomatic TB-pneumonia co-infection develop symptoms, respectively.
$\omega_1,\ \omega_2$	Rates at which individuals with symptomatic TB-pneumonia co-infection and asymptomatic TB-pneumonia co-infection recover from pneumonia, respectively.
$\phi_3,\ \phi_4$	Rates at which asymptomatic TB-pneumonia co-infected individuals undergoing treatment and symptomatic TB-pneumonia co-infected individuals undergoing treatment recover from pneumonia, respectively.
$\gamma_1,\ \gamma_2,\ \gamma_3,\ \gamma_4,\ \gamma_5,\ \gamma_6$	Mortality rates due to symptomatic TB disease; symptomatic TB-pneumonia co-infection; symptomatic TB-pneumonia co-infection during treatment; symptomatic TB during treatment; asymptomatic TB-pneumonia co-infection; and asymptomatic TB-pneumonia co-infection during treatment, respectively.
$\alpha_2,\ \alpha_3$	Rates at which individuals with asymptomatic TB and symptomatic TB recover during treatment, respectively.
n	An immunity parameter that delays the progression to severe tuberculosis disease.
κ	Rate at which individuals recovered from tuberculosis become susceptible again.
$\beta_1,\ \beta_2$	Transmission rates of pulmonary tuberculosis and pneumonia, respectively.
$\eta_1,\ \eta_2,\ \eta_3,\ \eta_4,\ \eta_5,\ \eta_6,\ \eta_7$	Transmission coefficients of tuberculosis from: symptomatic TB individuals; asymptomatic individuals co-infected with TB and pneumonia; asymptomatic TB individuals; symptomatic individuals co-infected with TB and pneumonia who are undergoing treatment; symptomatic TB individuals undergoing treatment; asymptomatic individuals co-infected with TB and pneumonia who are undergoing treatment; and asymptomatic TB individuals undergoing treatment, respectively.
$\chi_1,\ \chi_2,\ \chi_3$	Transmission coefficients of pneumonia from: asymptomatic individuals co-infected with TB and pneumonia; symptomatic individuals co-infected with TB and pneumonia who are undergoing treatment; and asymptomatic individuals co-infected with TB and pneumonia who are undergoing treatment, respectively.

The formulation of the new model is guided by the following assumptions:

1) Pneumonia is considered an opportunistic infection in individuals infected with pulmonary tuberculosis.
2) The vaccine is not 100% effective; therefore, some vaccinated individuals may still acquire infections.
3) The model does not include age structure; hence, vaccination is assumed to occur at birth.
4) Individuals undergoing treatment for co-infection with pulmonary tuberculosis and pneumonia recover from pneumonia first, as it is an acute disease.
5) Latently infected individuals do not transmit the infection.

Based on the variables, parameters, and assumptions, the schematic diagram illustrating the transmission dynamics of pulmonary tuberculosis in the presence of opportunistic pneumonia is presented in Figure 1.

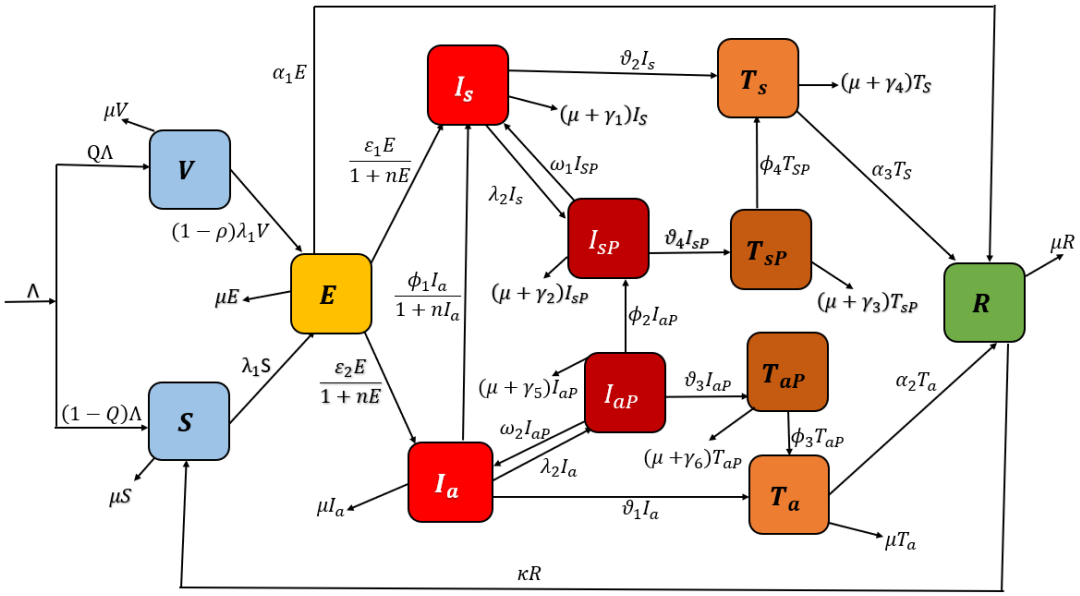

Figure 1. *Schematic diagram illustrating the transmission of pulmonary tuberculosis in the presence of opportunistic pneumonia.*

The transmission model is formulated as a system of ordinary differential equations, as follows:

$$\begin{cases} \frac{dS}{dt} = (1-Q)\Lambda + \kappa R - (\lambda_1 + \mu)S, \\ \frac{dV}{dt} = Q\Lambda - [(1-\rho)\lambda_1 + \mu]V, \\ \frac{dE}{dt} = \lambda_1 S + (1-\rho)\lambda_1 V - \left(\frac{\varepsilon_1}{1+nE} + \frac{\varepsilon_2}{1+nE} + \alpha_1 + \mu\right)E, \\ \frac{dI_a}{dt} = \frac{\varepsilon_2 E}{1+nE} + \omega_2 I_{aP} - (\lambda_2 + \frac{\phi_1}{1+nI_a} + \mu + \vartheta_1)I_a, \\ \frac{dI_S}{dt} = \frac{\varepsilon_1 E}{1+nE} + \frac{\phi_1 I_a}{1+nI_a} + \omega_1 I_{SP} - (\lambda_2 + \vartheta_2 + \mu + \gamma_1)I_S, \\ \frac{dI_{aP}}{dt} = \lambda_2 I_a - (\mu + \gamma_5 + \phi_2 + \vartheta_3 + \omega_2)I_{aP}, \\ \frac{dI_{SP}}{dt} = \lambda_2 I_S + \phi_2 I_{aP} - (\gamma_2 + \vartheta_4 + \mu + \omega_1)I_{SP}, \\ \frac{dT_a}{dt} = \vartheta_1 I_a + \phi_3 T_{aP} - (\mu + \alpha_2)T_a, \\ \frac{dT_S}{dt} = \vartheta_2 I_S + \phi_4 T_{SP} - (\mu + \gamma_4 + \alpha_3)T_S, \\ \frac{dT_{aP}}{dt} = \vartheta_3 I_{aP} - (\mu + \phi_3 + \gamma_6)T_{aP}, \\ \frac{dT_{SP}}{dt} = \vartheta_4 I_{SP} - (\mu + \phi_4 + \gamma_3)T_{SP}, \\ \frac{dR}{dt} = \alpha_1 E + \alpha_2 T_a + \alpha_3 T_S - (\mu + \kappa)R. \end{cases} \tag{1}$$

where λ_1 and λ_2 are defined as follows:

$$\lambda_1 = \beta_1(I_{SP} + \eta_1 I_S + \eta_2 I_{aP} + \eta_3 I_a + \eta_4 T_{SP} + \eta_5 T_S + \eta_6 T_{aP} + \eta_7 T_a)$$

$$\lambda_2 = \beta_2(I_{SP} + \chi_1 I_{aP} + \chi_2 T_{SP} + \chi_3 T_{aP})$$

It is noted that $\eta_7 < \eta_6 < \eta_5 < \eta_4 < \eta_3 < \eta_2 < \eta_1$ and $0 < \eta_1, \eta_2, \ldots, \eta_7 < 1$.
Similarly, $\chi_3 < \chi_2 < \chi_1$ and $0 < \chi_1, \chi_2, \chi_3 < 1$.
All parameters are assumed to be positive constants, and the initial conditions of system (1) are given as follows:

$$S(0) > 0,\ V(0) \geq 0,\ E(0) \geq 0,\ I_a(0) \geq 0,\ I_S(0) \geq 0,\ I_{aP}(0) \geq 0,\ I_{SP}(0) \geq 0,\ T_a(0) \geq 0,\ T_s(0) \geq 0,\ T_{aP}(t) \geq 0,\ T_{SP}(t) \geq 0, \text{ and } R(0) \geq 0. \quad (2)$$

3. Model Analysis

This section focuses on the analysis of model system (1) to identify the dynamics that influence the transmission of pulmonary tuberculosis in the presence of opportunistic pneumonia. The analysis addresses aspects such as the positivity and boundedness of solutions, equilibrium points, the reproduction number, and stability analysis.

3.1. Positivity of Solutions

The dynamical system (1) describes the changes in the human population. Therefore, it is necessary to prove that, given non-negative initial conditions, its solutions remain positive for $t > 0$, as demonstrated in Theorem 1.

Theorem 1: Given that the initial conditions $S(0)$, $V(0)$, $E(0)$, $I_a(0)$, $I_S(0)$, $I_{aP}(0)$, $I_{SP}(0)$, $T_a(0)$, $T_S(0)$, $T_{aP}(0)$, $T_{SP}(0)$ and $R(0)$ are non -negative, the solutions $S(t)$, $V(t)$, $E(t)$, $I_a(t)$, $I_S(t)$, $I_{aP}(t)$, $I_{SP}(t)$, $T_a(t)$, $T_S(t)$, $T_{aP}(t)$, $T_{SP}(t)$, and $R(t)$ remain positive for all $t > 0$.

Proof: The method of contradiction was used to demonstrate the positivity of solutions for all $0 < t < \infty$, under the condition that the initial values of the state variables are positive, as utilized by [30]. Suppose, at a given time, there exists a possibility such that:

t_1 is such that $S(t_1) = 0$ and $\dot{S}(t_1) < 0$, whenever

$$V(t) > 0,\ E(t) > 0,\ I_a(t) > 0,\ I_S(t) > 0,\ I_{aP}(t) > 0,\ I_{SP}(t) > 0,\ T_a(t) > 0,\ T_S(t) > 0,\ T_{aP}(t) > 0,\ T_{SP}(t) > 0 \text{ and } R(t) > 0 \text{ for } 0 < t < t_1. \quad (3)$$

Applying claim (3) to equation (1) of the system (1), yields:

$$\dot{S}(t_1) = (1 - Q)\Lambda + \kappa R(t_1) - (\lambda + \mu)S(t_1) \quad (4)$$

Since $S(t_1) = 0$, equation (4) becomes:

$$\dot{S}(t_1) = (1 - Q)\Lambda + \kappa R(t_1) > 0 \quad (5)$$

Equation (5) contradicts claim (3), which states that if $S(t_1) = 0$, then $\dot{S}(t_1) < 0$. Therefore, for t in the interval $0 < t < t_1$, we must have $S(t) > 0$, and thus t_1 can be extended to ∞.

Similarly, it can be shown that the solutions $V(t)$, $E(t)$, $I_a(t)$, $I_S(t)$, $I_{aP}(t)$, $I_{SP}(t)$, $T_a(t)$, $T_S(t)$, $T_{aP}(t)$, $T_{SP}(t)$, and $R(t)$ are non-negative.

Thus, the solutions set:

$$\{S(t), V(t), E(t), I_a(t), I_S(t), I_{aP}(t), I_{SP}(t), T_a(t), T_S(t), T_{aP}(t), T_{SP}(t), R(t)\} \geq 0 \ \forall\ t > 0. \quad (6)$$

This proves that the solutions of model system (1) remain positive for all $t > 0$.

3.2. Boundedness of Solutions

The model system (1) pertains to the human population; therefore, it is necessary to demonstrate that its solutions remain bounded for all $t > 0$. The following theorem is used to prove the boundedness of the solutions:

Theorem 2: Given the positive initial conditions, the feasible region is defined as:

$$\Omega = \left\{[S(t), V(t), E(t), I_a(t), I_S(t), I_{aP}(t), I_{SP}(t), T_a(t), T_S(t), T_{aP}(t), T_{SP}(t), R(t)] \in R_+^{12} : N \leq \frac{\Lambda}{\mu}\right\} \quad (7)$$

Proof: The sum of all equations in system (1) represents the total human population in the model and satisfies the following equation:

$$\frac{dN}{dt} = \Lambda - \mu N - \gamma_1 I_S - \gamma_2 I_{SP} - \gamma_3 T_{SP} - \gamma_4 T_S - \gamma_5 I_{aP} - \gamma_6 T_{aP} \quad (8)$$

In the absence of mortality due to tuberculosis infections, $\gamma_1 = \gamma_2 = \gamma_3 = \gamma_4 = 0$. Therefore, equation (8) simplifies to:

$$\frac{dN}{dt} = \Lambda - \mu N \tag{9}$$

Integrating equation (9) and applying the initial conditions yields:

$$N(t) = \frac{\Lambda}{\mu} + \left(N(0) - \frac{\Lambda}{\mu}\right) e^{-\mu t} \tag{10}$$

As $t \to \infty$, $N(t) \to \frac{\Lambda}{\mu}$, implying that $0 \leq N(t) \leq \frac{\Lambda}{\mu}$. Thus, the feasible solution of system (1) enters and remains in the region:

$$\Omega = \left\{[S(t), V(t), E(t), I_a(t), I_S(t), I_{aP}(t), I_{SP}(t), T_a(t), T_S(t), T_{aP}(t), T_{SP}(t), R(t)] \in R_+^{12} : N \leq \frac{\Lambda}{\mu}\right\} \tag{11}$$

Therefore, the basic model is well-posed both epidemiologically and mathematically, and it is sufficient to study its dynamics within the region Ω.

3.3. Disease Free Equilibrium Point and the Control Reproduction Number

The disease-free equilibrium point of system (1) is obtained by setting the latently infected class, all infectious classes, all treatment classes, and the recovered class to zero, i.e.,

$$E = I_a = I_S = I_{aP} = I_{SP} = T_a = T_S = T_{aP} = I_{SP} = R = 0.$$

Therefore, system (1) has a disease-free equilibrium given by:

$$B^0(S^0, V^0, E^0, I_a^0, I_S^0, I_{aP}^0, I_{SP}^0, T_a^0, T_S^0 \;\; T_{aP}^0, \;\; T_{SP}^0, \;\; R^0) = \left(\frac{(1-Q)\Lambda}{\mu}, \frac{Q\Lambda}{\mu}, 0,0,0,0,0,0,0,0,0\right) \tag{12}$$

The control reproduction number is defined as the expected number of secondary infections produced by a single infected individual during their entire infectious period in a population that is not entirely susceptible due to the presence of control measures [31]. The Next-Generation Matrix method, as described by [32], was used to compute the control reproduction number, which is determined as a spectral radius.

Let $X = (E, I_a, I_S, I_{aP}, I_{SP}, T_a, T_S, T_{aP}, T_{SP})^T$.
Then it follows from system (1) that:

$$\frac{dX}{dt} = f - v,$$

where f and v are matrices representing the new infection and transition terms, respectively, given by:

$$f = \begin{bmatrix} \lambda_1 S + (1-\rho)\lambda_1 V \\ 0 \\ 0 \\ 0 \\ 0 \\ 0 \\ 0 \\ 0 \\ 0 \end{bmatrix}, \quad v = \begin{bmatrix} \left(\frac{\varepsilon_1}{1+nE} + \frac{\varepsilon_2}{1+nE} + \alpha_1 + \mu\right) E \\ \left(\lambda_2 + \frac{\phi_1}{1+nI_a} + \mu + \vartheta_1\right) I_a - \frac{\varepsilon_2 E}{1+nE} - \omega_2 I_{aP} \\ (\lambda_2 + \vartheta_2 + \mu + \gamma_1) I_S - \frac{\varepsilon_1 E}{1+nE} - \frac{\phi_1 I_a}{1+nI_a} - \omega_1 I_{SP} \\ (\mu + \gamma_5 + \phi_2 + \vartheta_3 + \omega_2) I_{aP} - \lambda_2 I_a \\ (\gamma_2 + \vartheta_4 + \mu + \omega_1) I_{SP} - \phi_2 I_{aP} - \lambda_2 I_S \\ (\mu + \alpha_2) T_a - \vartheta_1 I_a - \phi_3 T_{aP} \\ (\mu + \gamma_4 + \alpha_3) T_S - \vartheta_2 I_S - \phi_4 T_{SP} \\ (\mu + \phi_3 + \gamma_6) T_{aP} - \vartheta_3 I_{aP} \\ (\mu + \phi_4 + \gamma_3) T_{SP} - \vartheta_4 I_{SP} \end{bmatrix}. \tag{13}$$

The Jacobian matrices associated with new infections (F) and transitions (V) at the disease-free equilibrium are given, respectively, by:

$$F=\begin{bmatrix}0 & \eta_3 a_1 & \eta_1 a_1 & \eta_2 a_1 & a_1 & \eta_7 a_1 & \eta_5 a_1 & \eta_6 a_1 & \eta_4 a_1\\ 0&0&0&0&0&0&0&0&0\\ 0&0&0&0&0&0&0&0&0\\ 0&0&0&0&0&0&0&0&0\\ 0&0&0&0&0&0&0&0&0\\ 0&0&0&0&0&0&0&0&0\\ 0&0&0&0&0&0&0&0&0\\ 0&0&0&0&0&0&0&0&0\\ 0&0&0&0&0&0&0&0&0\end{bmatrix}, \tag{14}$$

where: $a_1 = \beta_1[S^0 + (1-\rho)V^0]$.

The matrix V is given by:

$$V=\begin{bmatrix}h_1 & 0 & 0 & 0 & 0 & 0 & 0 & 0 & 0\\ -\varepsilon_2 & h_2 & 0 & -\omega_2 & 0 & 0 & 0 & 0 & 0\\ -\varepsilon_1 & -\phi_1 & h_3 & 0 & -\omega_1 & 0 & 0 & 0 & 0\\ 0 & 0 & 0 & h_4 & 0 & 0 & 0 & 0 & 0\\ 0 & 0 & 0 & -\phi_2 & h_5 & 0 & 0 & 0 & 0\\ 0 & -\vartheta_1 & 0 & 0 & 0 & h_6 & 0 & -\phi_3 & 0\\ 0 & 0 & -\vartheta_2 & 0 & 0 & 0 & h_7 & 0 & -\phi_4\\ 0 & 0 & 0 & -\vartheta_3 & 0 & 0 & 0 & h_8 & 0\\ 0 & 0 & 0 & 0 & -\vartheta_4 & 0 & 0 & 0 & h_9\end{bmatrix}. \tag{15}$$

where:
$h_1 = (\varepsilon_1 + \varepsilon_2 + \alpha_1 + \mu)$, $h_2 = (\phi_1 + \vartheta_1 + \mu)$, $h_3 = (\vartheta_2 + \gamma_1 + \mu)$, $h_4 = (\phi_2 + \gamma_5 + \vartheta_3 + \omega_2 + \mu)$, $h_5 = (\gamma_2 + \vartheta_4 + \omega_1 + \mu)$, $h_6 = (\mu + \alpha_2)$, $h_7 = (\mu + \gamma_4 + \alpha_3)$, $h_8 = (\mu + \phi_3 + \gamma_6)$, $h_9 = (\mu + \phi_4 + \gamma_3)$.

The dominant eigenvalue, corresponding to the spectral radius $\rho(FV^{-1})$, gives the control reproduction number, R_C, expressed as:

$$R_C = \frac{\beta_1\left[(\eta_3\varepsilon_2 h_3 + \eta_1\varepsilon_2\phi_1 + \eta_1\varepsilon_1 h_2)h_6 h_7 + \eta_7\vartheta_1\varepsilon_2 h_3 h_7 + \eta_5\vartheta_2 h_6(\varepsilon_2\phi_1 + \varepsilon_1 h_2)\right]\left[\frac{(1-Q)\Lambda}{\mu} + (1-\rho)\frac{Q\Lambda}{\mu}\right]}{h_1 h_2 h_3 h_6 h_7} \tag{16}$$

3.4. Local Stability of the Disease-Free Equilibrium

The local stability of the disease-free equilibrium is a critical aspect of analyzing the dynamics of infectious diseases within a population. This stability analysis helps determine whether small perturbations around the disease-free state cause the system to return to equilibrium or diverge towards disease prevalence. The following theorem illustrates the stability of the disease-free equilibrium point:

Theorem 3: The disease-free equilibrium point is locally asymptotically stable if $R_C < 1$, and unstable if $R_C > 1$.

Proof: To prove the local stability of the disease-free equilibrium, the Jacobian matrix of system (1), evaluated at the disease-free equilibrium point B^0, is derived as follows:

$$J(B^0)=\begin{bmatrix}-\mu & 0 & 0 & -c_1 & -c_2 & -c_3 & -\beta_1 S^0 & -c_4 & -c_5 & -c_6 & -c_7 & \kappa\\ 0 & -\mu & 0 & -c_8 & -c_9 & -c_{10} & -c_{11} & -c_{12} & -c_{13} & -c_{14} & -c_{15} & 0\\ 0 & 0 & -h_1 & d_1 & d_2 & d_3 & d_4 & d_5 & d_6 & d_7 & d_8 & 0\\ 0 & 0 & \varepsilon_2 & -h_2 & 0 & \omega_2 & 0 & 0 & 0 & 0 & 0 & 0\\ 0 & 0 & \varepsilon_1 & \phi_1 & -h_3 & 0 & \omega_1 & 0 & 0 & 0 & 0 & 0\\ 0 & 0 & 0 & 0 & 0 & -h_4 & 0 & 0 & 0 & 0 & 0 & 0\\ 0 & 0 & 0 & 0 & 0 & \phi_2 & -h_5 & 0 & 0 & 0 & 0 & 0\\ 0 & 0 & 0 & \vartheta_1 & 0 & 0 & 0 & -h_6 & 0 & \phi_3 & 0 & 0\\ 0 & 0 & 0 & 0 & \vartheta_2 & 0 & 0 & 0 & -h_7 & 0 & \phi_4 & 0\\ 0 & 0 & 0 & 0 & 0 & \vartheta_3 & 0 & 0 & 0 & -h_8 & 0 & 0\\ 0 & 0 & 0 & 0 & 0 & 0 & \vartheta_4 & 0 & 0 & 0 & -h_9 & 0\\ 0 & 0 & \alpha_1 & 0 & 0 & 0 & 0 & \alpha_2 & \alpha_3 & 0 & 0 & -h_{10}\end{bmatrix} \tag{17}$$

where: $c_1 = \beta_1\eta_3 S^0$, $c_2 = \beta_1\eta_1 S^0$, $c_3 = \beta_1\eta_2 S^0$, $c_4 = \beta_1\eta_7 S^0$, $c_5 = \beta_1\eta_5 S^0$, $c_6 = \beta_1\eta_6 S^0$, $c_7 = \beta_1\eta_4 S^0$, $c_8 = \beta_1(1-\rho)\eta_3 V^0$, $c_9 = \beta_1(1-\rho)\eta_1 V^0$, $c_{10} = \beta_1(1-\rho)\eta_2 V^0$, $c_{11} = \beta_1(1-\rho)V^0$, $c_{12} = \beta_1(1-\rho)\eta_7 V^0$, $c_{13} = \beta_1(1-\rho)\eta_5 V^0$, $c_{14} = \beta_1(1-\rho)\eta_6 V^0$, $c_{15} = \beta_1(1-\rho)\eta_4 V^0$, $d_1 = \beta_1\eta_3[S^0 + (1-\rho)V^0]$, $d_2 = \beta_1\eta_1[S^0 + (1-\rho)V^0]$, $d_3 = \beta_1\eta_2[S^0 + (1-\rho)V^0]$, $d_4 = \beta_1[S^0 + (1-\rho)V^0]$, $d_5 = \beta_1\eta_7[S^0 + (1-\rho)V^0]$, $d_6 = \beta_1\eta_5[S^0 + (1-\rho)V^0]$, $d_7 =$

$\beta_1\eta_6[S^0+(1-\rho)V^0]$, $d_8=\beta_1\eta_4[S^0+(1-\rho)V^0]$, $h_{10}=(\mu+\kappa)$.

The characteristic polynomial of equation (17) is given by:

$$(\mu+\lambda)(\mu+\lambda)(h_4+\lambda)(h_5+\lambda)(h_8+\lambda)(h_9+\lambda)(h_{10}+\lambda)(N_1\lambda^5+N_2\lambda^4+N_3\lambda^3+N_4\lambda^2+N_5\lambda+N_6)=0 \tag{18}$$

By the Routh-Hurwitz criterion, equation (18) has strictly negative roots, some of which are:

$$\lambda_1=\lambda_2=-\mu,\ \lambda_3=-h_4,\ \lambda_4=-h_5,\ \lambda_5=-h_8,\ \lambda_6=-h_9,\ \lambda_7=-h_{10}.$$

The remaining part of the characteristic polynomial in equation (18) is:

$$N_1\lambda^5+N_2\lambda^4+N_3\lambda^3+N_4\lambda^2+N_5\lambda+N_6=0 \tag{19}$$

Where N_1, N_2, N_3, N_4, N_5 and N_6 are determined as follows:

$$\begin{cases} N_1=1>0, \\ N_2=h_1+h_2+h_3+h_6+h_7, \\ N_3=h_7(h_1+h_2+h_3+h_6)+h_6(h_1+h_2+h_3)+h_3(h_1+h_2)+h_1h_2-d_1\varepsilon_2-d_2\varepsilon_1, \\ N_4=h_7[h_6(h_1+h_2+h_3)+h_3(h_1+h_2)+h_1h_2-(d_1\varepsilon_2+d_2\varepsilon_1)]+h_6[h_3(h_1+h_2)+h_1h_2-(d_1\varepsilon_2+d_2\varepsilon_1)] \\ \quad +h_3(h_1h_2-d_1\varepsilon_2)-h_2d_2\varepsilon_1-\phi_1d_2\varepsilon_2-\vartheta_1d_5\varepsilon_2-\vartheta_2d_6\varepsilon_1, \\ N_5=h_7[h_6h_3(h_1+h_2)+h_1h_2(h_3+h_6)-d_1\varepsilon_2(h_3+h_6)-d_2\phi_1\varepsilon_2-d_2\varepsilon_1(h_2+h_6)-d_5\vartheta_1\varepsilon_2] \\ \quad +h_6[h_3h_2h_1-d_1\varepsilon_2h_3-d_2\phi_1\varepsilon_2-d_2\varepsilon_1h_2-d_6\vartheta_2\varepsilon_1]-d_5\vartheta_1\varepsilon_2h_3-d_6\vartheta_2\varepsilon_1h_2-d_6\vartheta_2\phi_1\varepsilon_2, \\ N_6=h_1h_2h_3h_6h_7-[d_1\varepsilon_2h_3h_6h_7+d_2h_6h_7(\varepsilon_1h_2+\varepsilon_2\phi_1)+d_5\varepsilon_2\vartheta_1h_3h_7+d_6\vartheta_2h_6(\varepsilon_1h_2+\varepsilon_2\phi_1)]. \end{cases} \tag{20}$$

By the Routh-Hurwitz criterion, the following conditions must be satisfied:

$$N_1>0,\ N_2>0,\ N_3>0,\ N_4>0,\ N_5>0, \text{ and } N_6>0$$

From the condition $N_6>0$, we obtain:

$$h_1h_2h_3h_6h_7-[d_1\varepsilon_2h_3h_6h_7+d_2h_6h_7(\varepsilon_1h_2+\varepsilon_2\phi_1)+d_5\varepsilon_2\vartheta_1h_3h_7+d_6\vartheta_2h_6(\varepsilon_1h_2+\varepsilon_2\phi_1)]>0 \tag{21}$$

Inequality (21) can be rewritten as:

$$h_6h_7[d_1h_3\varepsilon_2+d_2(\varepsilon_1h_2+\varepsilon_2\phi_1)+d_5\varepsilon_2\vartheta_1h_3h_7+d_6\vartheta_2h_6(\varepsilon_1h_2+\varepsilon_2\phi_1)]<h_1h_2h_3h_6h_7 \tag{22}$$

Which implies:

$$\frac{h_6h_7[d_1h_3\varepsilon_2+d_2(\varepsilon_1h_2+\varepsilon_2\phi_1)+d_5\varepsilon_2\vartheta_1h_3h_7+d_6\vartheta_2h_6(\varepsilon_1h_2+\varepsilon_2\phi_1)]}{h_1h_2h_3h_6h_7}<1 \tag{23}$$

Substituting, $d_1=\beta_1\eta_3[S^0+(1-\rho)V^0]$, $d_2=\beta_1\eta_1[S^0+(1-\rho)V^0]$, $d_5=\beta_1\eta_7[S^0+(1-\rho)V^0]$, $d_6=\beta_1\eta_5[S^0+(1-\rho)V^0]$, $S^0=(1-Q)\frac{\Lambda}{\mu}$ and $V^0=\frac{Q\Lambda}{\mu}$ into inequality (23), and rearranging yields:

$$\frac{\beta_1\left[(\eta_3\varepsilon_2h_3+\eta_1\varepsilon_2\phi_1+\eta_1\varepsilon_1h_2)h_6h_7+\eta_7\vartheta_1\varepsilon_2h_3h_7+\eta_5\vartheta_2h_6(\varepsilon_2\phi_1+\varepsilon_1h_2)\right]\left[\frac{(1-Q)\Lambda}{\mu}+(1-\rho)\frac{Q\Lambda}{\mu}\right]}{h_1h_2h_3h_6h_7}<1 \tag{24}$$

However, the left-hand side of equation (24) defines the control reproduction number:

$$\frac{\beta_1\left[(\eta_3\varepsilon_2h_3+\eta_1\varepsilon_2\phi_1+\eta_1\varepsilon_1h_2)h_6h_7+\eta_7\vartheta_1\varepsilon_2h_3h_7+\eta_5\vartheta_2h_6(\varepsilon_2\phi_1+\varepsilon_1h_2)\right]\left[\frac{(1-Q)\Lambda}{\mu}+(1-\rho)\frac{Q\Lambda}{\mu}\right]}{h_1h_2h_3h_6h_7}=R_C \tag{25}$$

Therefore, equation (24) can be written as follows:

$$R_C<1. \tag{26}$$

From equation (26), the disease-free equilibrium is locally asymptotically stable if $R_C<1$. This implies that each infectious individual infects, on average, less than one susceptible individual during the infectious period, leading to the

eventual elimination of the disease.

3.5. The Endemic Equilibrium

The steady state at which pulmonary tuberculosis persists in the presence of opportunistic pneumonia within the community is referred to as the endemic equilibrium of system (1). At this equilibrium, the rate of change of the population in each class is zero. Hence, the model system (1) can be represented as:

$$\begin{cases} 0 = (1-Q)\Lambda + \kappa R - (\lambda_1 + \mu)S, \\ 0 = Q\Lambda - [(1-\rho)\lambda_1 + \mu]V, \\ 0 = \lambda_1 S + (1-\rho)\lambda_1 V - \left(\frac{\varepsilon_1}{1+nE} + \frac{\varepsilon_2}{1+nE} + \alpha_1 + \mu\right)E, \\ 0 = \frac{\varepsilon_2 E}{1+nE} + \omega_2 I_{aP} - (\lambda_2 + \frac{\phi_1}{1+nI_a} + \mu + \vartheta_1)I_a, \\ 0 = \frac{\varepsilon_1 E}{1+nE} + \frac{\phi_1 I_a}{1+nI_a} + \omega_1 I_{SP} - (\lambda_2 + \vartheta_2 + \mu + \gamma_1)I_S, \\ 0 = \lambda_2 I_a - (\mu + \gamma_5 + \phi_2 + \vartheta_3 + \omega_2)I_{aP}, \\ 0 = \lambda_2 I_S + \phi_2 I_{aP} - (\gamma_2 + \vartheta_4 + \mu + \omega_1)I_{SP}, \\ 0 = \vartheta_1 I_a + \phi_3 T_{aP} - (\mu + \alpha_2)T_a, \\ 0 = \vartheta_2 I_S + \phi_4 T_{SP} - (\mu + \gamma_4 + \alpha_3)T_S, \\ 0 = \vartheta_3 I_{aP} - (\mu + \phi_3 + \gamma_6)T_{aP}, \\ 0 = \vartheta_4 I_{SP} - (\mu + \phi_4 + \gamma_3)T_{SP}, \\ 0 = \alpha_1 E + \alpha_2 T_a + \alpha_3 T_S - (\mu + \kappa)R. \end{cases} \tag{27}$$

The steady-state solution for system (27) is given by:

$$B^* = (S^*, V^*, E^*, I_a^*, I_S^*, I_{aP}^*, I_{SP}^*, T_a^*, T_S^*, T_{aP}^*, T_{SP}^*, R^*)$$

where:

$S^* = \frac{(1-Q)\Lambda + \kappa R^*}{\lambda_1^{**} + \mu}$,

$V^* \frac{Q\Lambda}{(1-\rho)\lambda_1^{**} + \mu}$,

$E^* = \frac{\lambda_1^{**}[((1-\rho)\lambda_1^{**} + \mu)((1-Q)\Lambda + \kappa R^*) + (\lambda_1^{**} + \mu)(1-\rho)Q\Lambda]}{(\lambda_1^{**} + \mu)(\sigma_1 + \sigma_2 + \vartheta_1 + \mu)((1-\rho)\lambda_1^{**} + \mu)}$,

$I_a^* = \frac{\lambda_1^{**}\sigma_2(\mu + \gamma_5 + \phi_2 + \vartheta_3 + \omega_2)[((1-\rho)\lambda_1^{**} + \mu)((1-Q)\Lambda + \kappa R^*) + (\lambda_1^{**} + \mu)(1-\rho)Q\Lambda]}{[(\mu + \gamma_5 + \phi_2 + \vartheta_3 + \omega_2)(\lambda_2 + \sigma_3 + \mu + \vartheta_1) - \lambda_2^{**}](\lambda_1^{**} + \mu)(\sigma_1 + \sigma_2 + \vartheta_1 + \mu)((1-\rho)\lambda_1^{**} + \mu)}$,

$I_S^* = \frac{D_1 D_2(\mu + \gamma_5 + \phi_2 + \vartheta_3 + \omega_2)}{[(\mu + \gamma_5 + \phi_2 + \vartheta_3 + \omega_2)(\lambda_2^{**} + \sigma_3 + \mu + \vartheta_1) - \lambda_2^{**}][(\lambda_2^{**} + \vartheta_2 + \mu + \gamma_1)(\gamma_2 + \vartheta_4 + \mu + \omega_1) - \omega_1\lambda_2^{**}]A_1}$,

$I_{aP}^* = \frac{D_1\lambda_2^{**}\sigma_2(\mu + \gamma_5 + \phi_2 + \vartheta_3 + \omega_2)}{[(\mu + \gamma_5 + \phi_2 + \vartheta_3 + \omega_2)(\lambda_2^{**} + \sigma_3 + \mu + \vartheta_1) - \lambda_2^{**}](\mu + \gamma_5 + \phi_2 + \vartheta_3 + \omega_2)A_1}$,

$I_{SP}^* = \frac{\lambda_2^{**}(\mu + \gamma_5 + \phi_2 + \vartheta_3 + \omega_2)D_1[(\mu + \gamma_5 + \phi_2 + \vartheta_3 + \omega_2)D_2 + D_3\phi_2\sigma_2]}{[(\mu + \gamma_5 + \phi_2 + \vartheta_3 + \omega_2)(\lambda_2^{**} + \sigma_3 + \mu + \vartheta_1) - \lambda_2^{**}](\mu + \gamma_5 + \phi_2 + \vartheta_3 + \omega_2)(\gamma_2 + \vartheta_4 + \mu + \omega_1)D_3A_1}$,

$T_a^* = \frac{D_1\sigma_2(\mu + \gamma_5 + \phi_2 + \vartheta_3 + \omega_2)[\vartheta_1(\mu + \gamma_5 + \phi_2 + \vartheta_3 + \omega_2)(\mu + \phi_3 + \gamma_6) + \phi_3\vartheta_3\lambda_2^{**}]}{(\alpha_2 + \mu)(\mu + \gamma_5 + \phi_2 + \vartheta_3 + \omega_2)(\mu + \phi_3 + \gamma_6)D_4A_1}$,

$T_S^* = \frac{D_1(\mu + \gamma_5 + \phi_2 + \vartheta_3 + \omega_2)[\vartheta_2 D_2(\mu + \gamma_5 + \phi_2 + \vartheta_3 + \omega_2)(\gamma_2 + \vartheta_4 + \mu + \omega_1)(\mu + \phi_3 + \gamma_6) + \phi_4\vartheta_4\lambda_2^{**}D_5]}{(\mu + \gamma_5 + \phi_2 + \vartheta_3 + \omega_2)(\gamma_2 + \vartheta_4 + \mu + \omega_1)(\mu + \phi_3 + \gamma_6)(\gamma_4 + \alpha_3 + \mu)D_3D_4A_1}$,

$T_{aP}^* = \frac{\vartheta_3 D_1\lambda_2^{**}\sigma_2(\mu + \gamma_5 + \phi_2 + \vartheta_3 + \omega_2)}{[(\mu + \gamma_5 + \phi_2 + \vartheta_3 + \omega_2)(\lambda_2^{**} + \sigma_3 + \mu + \vartheta_1) - \lambda_2^{**}](\mu + \gamma_5 + \phi_2 + \vartheta_3 + \omega_2)(\mu + \phi_3 + \gamma_6)A_1}$,

$T_{SP}^* = \frac{\vartheta_4\lambda_2^{**}(\mu + \gamma_5 + \phi_2 + \vartheta_3 + \omega_2)D_1[(\mu + \gamma_5 + \phi_2 + \vartheta_3 + \omega_2)D_2 + D_3\phi_2\sigma_2]}{[(\mu + \gamma_5 + \phi_2 + \vartheta_3 + \omega_2)(\lambda_2^{**} + \sigma_3 + \mu + \vartheta_1) - \lambda_2^{**}](\mu + \gamma_5 + \phi_2 + \vartheta_3 + \omega_2)(\gamma_2 + \vartheta_4 + \mu + \omega_1)(\mu + \phi_4 + \gamma_3)D_3A_1}$,

$R^* = \frac{\lambda_1^{**}[((1-\rho)\lambda_1^{**} + \mu)S^* + (\lambda_1^{**} + \mu)(1-\rho)Q\Lambda](\alpha_1 D_6 + \alpha_2 D_7 + \alpha_3 D_8)}{(\mu + \gamma_5 + \phi_2 + \vartheta_3 + \omega_2)(\gamma_2 + \vartheta_4 + \mu + \omega_1)(\mu + \phi_3 + \gamma_6)D_3D_4A_2A_3A_4A_5}$.

Here,

$A_1 = (\lambda_1^{**} + \mu)(\sigma_1 + \sigma_2 + \vartheta_1 + \mu)((1-\rho)\lambda_1^{**} + \mu)$,

$A_2 = (\sigma_1 + \sigma_2 + \vartheta_1 + \mu)((1-\rho)\lambda_1^{**} + \mu)$, $A_3 = (\mu + \alpha_2)$,

$A_4 = (\mu + \gamma_4 + \alpha_3)$, $A_5 = (\kappa + \mu)$,

$D_1 = \lambda_1^{**}\left[((1-\rho)\lambda_1^{**} + \mu)\left((1-Q)\Lambda + \kappa R^*\right) + (\lambda_1^{**} + \mu)(1-\rho)Q\Lambda\right]$,

$D_2 = \left(\left((\lambda_2 + \sigma_3 + \mu + \vartheta_1) - \lambda_2^{**}\right) + \sigma_3\sigma_2\right)(\gamma_2 + \vartheta_4 + \mu + \omega_1) + \sigma_2\omega_1\sigma_3$,

$D_3 = (\lambda_2^{**} + \vartheta_2 + \mu + \gamma_1)(\gamma_2 + \vartheta_4 + \mu + \omega_1) - \omega_1\lambda_2^{**}$,

$D_4 = (\mu + \gamma_5 + \phi_2 + \vartheta_3 + \omega_2)(\lambda_2^{**} + \sigma_3 + \mu + \vartheta_1) - \lambda_2^{**}$,

$D_5 = (\mu + \gamma_5 + \phi_2 + \vartheta_3 + \omega_2)D_2 + D_3\phi_2\sigma_2$,

$D_6 = (\mu + \gamma_5 + \phi_2 + \vartheta_3 + \omega_2)(\gamma_2 + \vartheta_4 + \mu + \omega_1)(\mu + \phi_3 + \gamma_6)D_3D_4A_2A_3$,

$D_7 = \sigma_2(\gamma_2 + \vartheta_4 + \mu + \omega_1)(\mu + \gamma_5 + \phi_2 + \vartheta_3 + \omega_2)[\vartheta_1(\mu + \gamma_5 + \phi_2 + \vartheta_3 + \omega_2)(\mu + \phi_3 + \gamma_6) + \phi_3\vartheta_3\lambda_2^{**}]D_3D_4A_1A_3$,

$D_8 = (\mu + \gamma_5 + \phi_2 + \vartheta_3 + \omega_2)[\vartheta_2 D_2(\mu + \gamma_5 + \phi_2 + \vartheta_3 + \omega_2)(\gamma_2 + \vartheta_4 + \mu + \omega_1)(\mu + \phi_3 + \gamma_6) + \phi_4\vartheta_4\lambda_2^{**}D_5]A_2$,

$\sigma_1 = \frac{\varepsilon_1}{1+nE}$,

$\sigma_2 = \frac{\varepsilon_2}{1+nE}$,
$\sigma_3 = \frac{\phi_1}{1+nI_a}$.

3.6. Global Stability of the Endemic Equilibrium

In epidemiological modeling, the global stability of an endemic equilibrium implies that the disease will persist at a constant level over time, regardless of the initial state of the population, provided the initial conditions lie within a realistic and meaningful range. This concept is crucial for understanding the long-term dynamics of disease transmission and for designing effective public health strategies.

To prove the global asymptotic stability of the endemic equilibrium, the method of Lyapunov functions is employed. A logarithmic Lyapunov function used for this purpose is defined as follows:

$$L(S,V,E,I_a,I_S,I_{aP},I_{SP},T_a,T_{SP},T_{aP},T_{SP},R) = \left(S - S^* + S^* ln\frac{S^*}{S}\right) + \left(V - V^* + V^* ln\frac{V^*}{V}\right) + \left(E - E^* + E^* ln\frac{E^*}{E}\right) + \left(I_a - I_a^* + I_a^* ln\frac{I_a^*}{I_a}\right) + \left(I_s - I_s^* + I_s^* ln\frac{I_S^*}{I_s}\right) + \left(I_{aP} - I_{aP}^* + I_{aP}^* ln\frac{I_{aP}^*}{I_{aP}}\right) + \left(I_{SP} - I_{SP}^* + I_{SP}^* ln\frac{I_{SP}^*}{I_{SP}}\right) + \left(I_{SP} - I_{SP}^* + I_{SP}^* ln\frac{I_{SP}^*}{I_{SP}}\right) + \left(T_a - T_a^* + T_a^* ln\frac{T_a^*}{T_a}\right) + \left(T_s - T_s^* + T_s^* ln\frac{T_S^*}{T_s}\right) + \left(T_{aP} - T_{aP}^* + T_{aP}^* ln\frac{T_{aP}^*}{T_{aP}}\right) + \left(T_{SP} - T_{SP}^* + T_{SP}^* ln\frac{T_{SP}^*}{T_{SP}}\right) + \left(R - R^* + ln\frac{R^*}{R}\right) \quad (28)$$

The derivative of L along the solution trajectories of system (1) is given by:

$$\frac{dL}{dt} = \left(\frac{S-S^*}{S}\right)\frac{dS}{dt} + \left(\frac{V-V^*}{V}\right)\frac{dV}{dt} + \left(\frac{E-E^*}{E}\right)\frac{dE}{dt} + \left(\frac{I_a-I_a^*}{I_a}\right)\frac{dI_a}{dt} + \left(\frac{I_s-I_s^*}{I_s}\right)\frac{dI_s}{dt} + \left(\frac{I_{aP}-I_{aP}^*}{I_{aP}}\right)\frac{dI_{aP}}{dt} + \left(\frac{I_{SP}-I_{SP}^*}{I_{SP}}\right)\frac{dI_{SP}}{dt} + \left(\frac{T_a-T_a^*}{T_a}\right)\frac{dT_a}{dt} + \left(\frac{T_s-T_s^*}{T_s}\right)\frac{dT_s}{dt} + \left(\frac{T_{aP}-T_{aP}^*}{T_{aP}}\right)\frac{dI_{aP}}{dt} + \left(\frac{T_{SP}-T_{SP}^*}{T_{SP}}\right)\frac{dI_{SP}}{dt} + \left(\frac{R-R^*}{R}\right)\frac{dR}{dt} \quad (29)$$

Substituting the expressions for $\frac{dS}{dt}, \frac{dV}{dt}, \frac{dE}{dt}, \frac{dI_a}{dt}, \frac{dI_s}{dt}, \frac{dI_{aP}}{dt}, \frac{dI_{SP}}{dt}, \frac{dT_a}{dt}, \frac{dT_s}{dt}, \frac{dT_{aP}}{dt}, \frac{dT_{SP}}{dt}, \frac{dR}{dt}$ from model system (1) into equation (29) and simplifying yields:

$$\frac{dL}{dt} = K - Y \quad (30)$$

where:

$$K = \Lambda + \kappa R + \frac{\kappa R^* S^*}{S} + \frac{\lambda_1 S^* E^*}{E} + (1-\rho)\lambda_1 V + \frac{(1-\rho)\lambda_1 V^* E^*}{E} + \sigma_2 E + \frac{\sigma_2 I_a^* E^*}{I_a} + \sigma_1 E + \frac{\sigma_1 I_S^* E^*}{I_s} + \sigma_3 I_a + \frac{\sigma_3 I_S^* I_a^*}{I_s} + \lambda_2 I_a + \frac{\lambda_2 I_{aP}^* I_a^*}{I_{aP}} + \lambda_2 I_S + \frac{\lambda_2 I_{SP}^* I_S^*}{I_{SP}} + \phi_2 I_{aP} + \frac{\phi_2 I_{SP}^* I_{aP}^*}{I_{SP}} + \vartheta_1 I_a + \frac{\vartheta_1 I_a^* T_a^*}{T_a} + \phi_3 T_{aP} + \frac{\phi_3 T_a^* T_{aP}^*}{T_a} + \vartheta_2 I_s + \frac{\vartheta_2 I_S^* T_S^*}{T_s} + \phi_4 T_{aP} + \frac{\phi_4 T_S^* T_{aP}^*}{T_S} + \vartheta_3 I_{aP} + \frac{\vartheta_3 T_{aP}^* I_{aP}^*}{T_{aP}} + \vartheta_4 I_{SP} + \frac{\vartheta_4 T_{SP}^* I_{SP}^*}{T_{SP}} + \alpha_1 E + \frac{\alpha_1 E^* R^*}{R} + \alpha_2 T_a + \frac{\alpha_2 T_a^* R^*}{R} + \alpha_3 T_s + \frac{\alpha_3 T_S^* R^*}{R} + \frac{\Lambda Q V^*}{V} + \lambda_1 S$$

$$Y = \frac{\Lambda S^*}{S} + \frac{\Lambda Q S^*}{S} + \frac{\kappa R S^*}{S} + \frac{\lambda_1 S E^*}{E} + (1-\rho)\lambda_1 V^* + \frac{(1-\rho)\lambda_1 E^*}{E^*} + \sigma_2 E^* + \frac{\sigma_2 E I_a^*}{I_a} + \sigma_1 E^* + \frac{\sigma_1 E I_S^*}{I_S} + \sigma_3 I_a^* + \frac{\sigma_3 I_a I_S^*}{I_s} + \lambda_2 I_a^* + \frac{\lambda_2 I_{aP}^* I_a}{I_{aP}} + \lambda_2 I_S^* + \frac{\lambda_2 I_{SP}^* I_S}{I_{SP}} + \phi_2 I_{aP}^* + \frac{\phi_2 I_{SP}^* I_{aP}}{I_{SP}} + \vartheta_1 I_a^* + \frac{\vartheta_1 I_a T_a^*}{T_a} + \phi_3 T_{aP}^* + \frac{\phi_3 T_a^* T_{aP}}{T_a} + \vartheta_2 I_S^* + \frac{\vartheta_2 I_S T_S^*}{T_s} + \phi_4 T_{aP}^* + \frac{\phi_4 T_S^* T_{aP}}{T_S} + \alpha_1 E^* + \frac{\alpha_1 E R^*}{R} + \alpha_2 T_a^* + \frac{\alpha_2 T_a R^*}{R} + \alpha_3 T_S^* + \frac{\alpha_3 T_S R^*}{R} + \lambda_1 S^* + \frac{(S-S^*)^2}{S}[\lambda_1 + \mu] + \frac{(V-V^*)^2}{V}[(1-\rho)\lambda_1 + \mu] + \frac{(E-E^*)^2}{E}[\sigma_2 + \sigma_1 + \alpha_1 + \mu] + \frac{(I_a-I_a^*)^2}{I_a}[\vartheta_1 + \sigma_3 + \lambda_2 + \mu] + \frac{(I_S-I_S^*)^2}{I_s}[\vartheta_2 + \gamma_1 + \lambda_2 + \mu] + \frac{(I_{aP}-I_{aP}^*)^2}{I_{aP}}[\phi_2 + \gamma_5 + \vartheta_3 + \mu + \omega_2] + \frac{(I_{SP}-I_{SP}^*)^2}{I_{SP}}[\gamma_2 + \vartheta_4 + \mu + \omega_1] + \frac{(T_a-T_a^*)}{T_a}[\alpha_2 + \mu] + \frac{(T_S-T_S^*)^2}{T_s}[\gamma_4 + \alpha_3 + \mu] + \frac{(T_{aP}-T_{aP}^*)^2}{T_{aP}}[\mu + \phi_3 + \gamma_6] + \frac{(T_{SP}-T_{SP}^*)^2}{T_{SP}}[\mu + \phi_4 + \gamma_3] + \frac{(R-R^*)^2}{R}[\kappa + \mu]$$

If $K \leq Y$, then $\frac{dL}{dt} \leq 0$, and $\frac{dL}{dt} = 0$ if and only if

$$S = S^*, V = V^*, E = E^*, \ I_a = I_a^*, I_s = I_s^*, I_{aP} = I_{aP}^*, I_{SP} = I_{SP}^*, T_a = T_a^*, T_s = T_s^*, T_{aP} = T_{aP}^*, T_{aP} = T_{aP}^*, T_{SP} = T_{SP}^*, R = R^*.$$

Therefore, the largest compact invariant set in $\left\{(S^*, V^*, E^*, I_a^*, I_S^*, I_{aP}^*, I_{SP}^*, T_a^*, T_S^*, T_{aP}^*, T_{SP}^*, R^*) \in \Omega : \frac{dL}{dt} = 0\right\}$ is the singleton endemic equilibrium point B*. Thus, by LaSalle's invariance principle [33], it follows that as $t \to \infty$, the solution of the model system (1) approaches the endemic equilibrium B^* when the control reproduction number $R_C^* > 1$.

Therefore, the endemic equilibrium point B^* is globally asymptotically stable in the invariant set Ω if $K < Y$.

3.7. Sensitivity Analysis of the Control Reproduction Number

In this section, a sensitivity analysis of the reproduction number is presented to assess the relative importance of various parameters influencing the transmission and prevalence of pulmonary tuberculosis and opportunistic pneumonia within the population. The normalized forward sensitivity index, as described in [34], is employed for this analysis. This index measures the relative change in the control reproduction number R_C with respect to a given parameter m and is defined as:

$$\Upsilon_m^{R_C} = \frac{\partial R_C}{\partial m} \times \frac{m}{R_C} \tag{31}$$

The parameter values in Table 3 are used to calculate the sensitivity indices of R_C with respect to the parameters β_1, α_1, α_2, α_3, ε_1, ε_2, ϑ_1, ϑ_2, ρ, η_1, η_3, and ϕ_1.

Table 3. *Baseline parameter values used in the tuberculosis-pneumonia co-infection model.*

Parameter	Value	Reference
Λ	1508563 $year^{-1}$	[36]
Q	0.8 $year^{-1}$	[36]
ρ	0.6	[1]
μ	0.0057 $year^{-1}$	[36]
ε_1, ε_2	0.7, 0.3 $year^{-1}$	[37]
ϑ_1, ϑ_2	0.6, 0.8 $year^{-1}$	[37]
ϑ_3, ϑ_4	0.68, 0.053 $year^{-1}$	Data fitted
n	0.0003 $year^{-1}$	Data fitted
γ_1, γ_2	0.1, 0.06 $year^{-1}$	[38]
γ_3	0.031 $year^{-1}$	Data fitted
γ_4	0.03 $year^{-1}$	[38]
γ_5, γ_6	0.0004, 0.03 $year^{-1}$	Data fitted
α_1, α_2	0.5, 0.1 $year^{-1}$	[39]
α_3	0.0153 $year^{-1}$	[40]
ϕ_1	0.038 $year^{-1}$	[40]
ϕ_2	0.0123 $year^{-1}$	Data fitted
ϕ_3, ϕ_4	0.001, 0.00219 $year^{-1}$	[2]
κ	0.003 $year^{-1}$	[2]
β_1	2.2258×10^{-7}	[38]
β_2	1.179684×10^{-7}	[38]
ω_1, ω_2	0.001, 0.001$year^{-1}$	Data fitted
χ_1, χ_2, χ_3	0.6012, 0.0576, 0.0315	Data fitted
η_1, η_2, η_3	0.37048, 0.1655, 0.1527	Data fitted
η_4, η_5	0.1487, 0.13895	Data fitted
η_6, η_7	0.10543, 0.0678	Data fitted

The computed sensitivity indices are presented in Table 4. A positive sensitivity index indicates that the reproduction number increases with an increase in the corresponding parameter, while a negative sensitivity index indicates that the reproduction

number decreases as the parameter increases [35].

From Table 4, it is observed that the parameters β_1, ε_1, ε_2, η_1, η_3, and ϕ_1 have positive sensitivity index values, indicating that an increase in these parameters leads to a corresponding increase in the number of infected individuals. On the other hand, ϑ_1, ϑ_2, α_1,α_2, α_3, and ρ have negative sensitivity index values, meaning that increasing these parameters results in a decrease in the number of infected individuals. For instance, if the transmission rate β_1 increases by 10%, the reproduction number also increases by 10%. Conversely, increasing the screening rate ϑ_1 for asymptomatic pulmonary tuberculosis individuals by 10% reduces R_C by approximately 0.44314%, while increasing the vaccine efficacy ρ by 10% decreases R_C by approximately 9.23077%.

Table 4. *Sensitivity indices of the control reproduction number relative to selected model parameters.*

Parameter	Sensitivity index
β_1	+1
ε_1	+0.40281
η_1	+0.129267
ε_2	+0.066953
η_3	+0.031342
ϕ_1	+0.014144
ϑ_1	−0.044314
ϑ_2	−0.025438
α_1	−0.332071
α_2	−0.074734
α_3	−0.074734
ρ	−0.923077

4. Model Simulations

Numerical simulations of the system of model equations (1) were conducted to predict the epidemic behavior of pulmonary tuberculosis in the presence of opportunistic pneumonia. These simulations were performed utilizing MATLAB's built-in ordinary differential equation solver, ode45. The parameter values used are provided in Table 3, and the initial state values are as follows:

$S(0 = 5{,}062{,}291$; $V(0) = 22{,}780{,}311$; $E(0) = 1{,}687{,}405$; $I_a(0) = 30{,}364$; $I_S(0) = 41{,}733$; $I_{aP}(0) = 26{,}588$; $I_{SP} = 41{,}253$; $T_a(0) = 10{,}167$; $T_S(0) = 21{,}787$; $T_{aP} = 39{,}738$; $T_{SP} = 27{,}427$; and $R(0) = 5{,}705{,}328$. These values were obtained from published Kenyan data [2, 36-40].

The simulations are conducted over a time span of 0 to 20 years, taking into account that pulmonary tuberculosis infections often take a long time to reactivate into chronic disease and eventually be cured. The simulation results are presented graphically in Figures 2-10.

4.1. Effects of Varying the Immunity Parameter on Co-Infected Populations

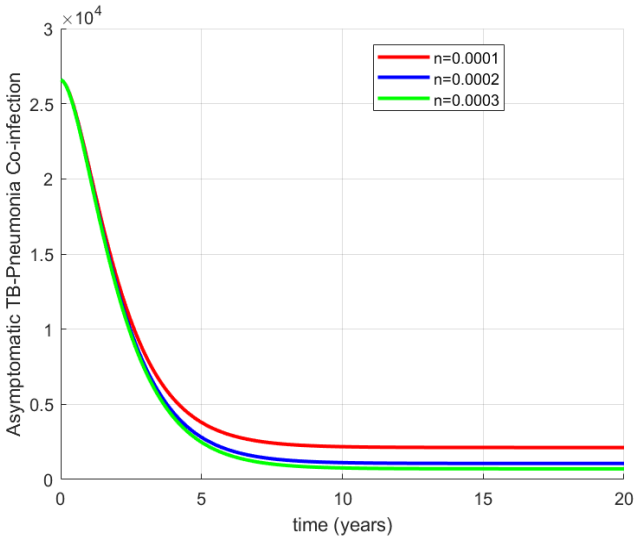

Figure 2. *Effects of varying the immunity parameter* (n) *on asymptomatic tuberculosis-pneumonia co-infections.*

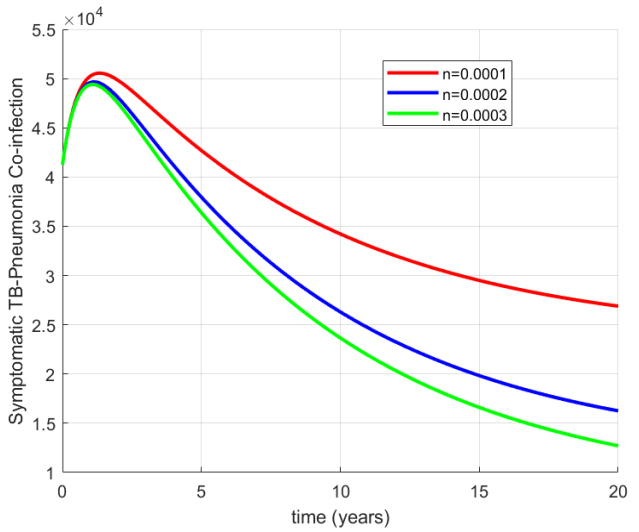

Figure 3. *Effects of varying the immunity parameter* (n) *on symptomatic tuberculosis-pneumonia co-infections.*

In the model flow chart shown in Figure 1, n represents the natural immunity parameter. Figures 2 and 3 illustrate the effects of varying this parameter on tuberculosis-pneumonia co-infections. An increase in the natural immunity parameter is observed to reduce the number of co-infected individuals.

This reduction occurs because enhanced natural immunity diminishes infection transmission by slowing the progression of latent tuberculosis infections to active pulmonary tuberculosis disease, thereby significantly lowering the number of individuals co-infected with pulmonary tuberculosis and opportunistic pneumonia.

4.2. Effects of Varying the Screening Rate of Asymptomatic Pulmonary Tuberculosis Patients on Co-Infected Populations

In the flow chart depicted in Figure 1, ϑ_1 represents the screening rate for individuals with asymptomatic infectious tuberculosis. Figure 4 illustrates the effects of screening these individuals on the population with severe tuberculosis-pneumonia co-infections. An increase in the screening rate for asymptomatic infectious individuals is observed to decrease the number of people with severe tuberculosis-pneumonia co-infections. This decrease is attributed to a reduction in the continuous transmission of pulmonary tuberculosis from undetected asymptomatic carriers and a decreased progression from the asymptomatic infectious stage to severe pulmonary tuberculosis. Consequently, the transmission rate declines, resulting in fewer individuals becoming co-infected with tuberculosis and opportunistic pneumonia.

4.3. Effects of Varying the Treatment Rate of Pulmonary Tuberculosis on Co-Infected Populations

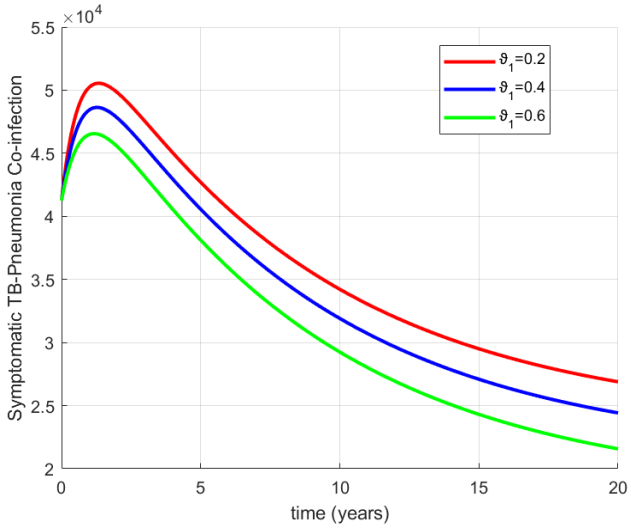

Figure 4. *Effects of varying the screening rate* (ϑ_1) *for asymptomatic tuberculosis individuals on co-infection.*

According to the model flow chart in Figure 1, ϑ_2 represents the treatment rate for individuals with severe pulmonary tuberculosis. Figures 5 and 6 illustrate the effects of varying this treatment rate on tuberculosis-pneumonia co-infections. An increase in the treatment rate of pulmonary tuberculosis is observed to reduce the number of co-infections. This reduction is attributed to the decreased transmission of infection resulting from effective treatment, which subsequently lowers the number of individuals co-infected with pulmonary tuberculosis and opportunistic pneumonia.

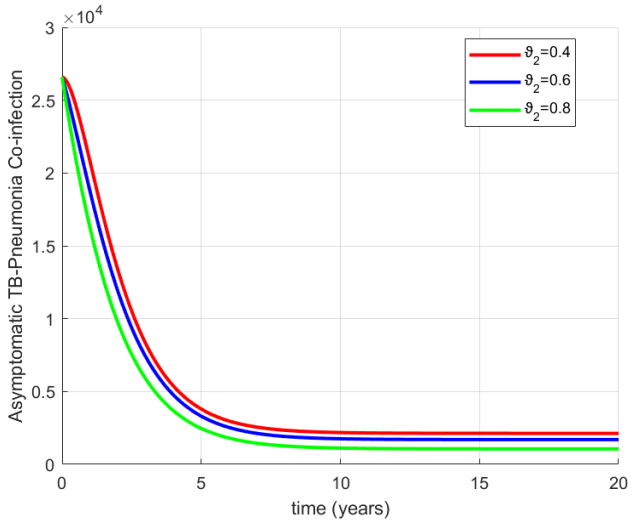

Figure 5. *Effects of varying the treatment rate* (ϑ_2) *for tuberculosis on asymptomatic tuberculosis-pneumonia co-infection.*

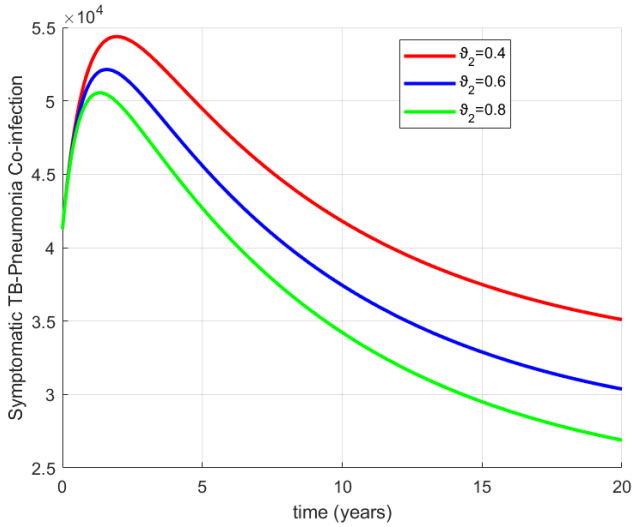

Figure 6. *Effects of varying the treatment rate* (ϑ_2) *for tuberculosis on symptomatic tuberculosis-pneumonia co-infection.*

4.4. Effects of Varying Vaccine Efficacy on Co-Infected Populations

According to the model flow chart in Figure 1, ρ represents the efficacy of the pulmonary tuberculosis vaccine. Figures 7 and 8 illustrate the effects of varying vaccine efficacy on populations co-infected with pulmonary tuberculosis

and pneumonia. The simulations predict that an increase in vaccine efficacy reduces the number of individuals co-infected with tuberculosis and opportunistic pneumonia. This reduction is attributed to enhanced immunity provided by a more effective vaccine, which decreases the proportion of the population infected with pulmonary tuberculosis and, consequently, significantly reduces the number of individuals co-infected with both pulmonary tuberculosis and opportunistic pneumonia.

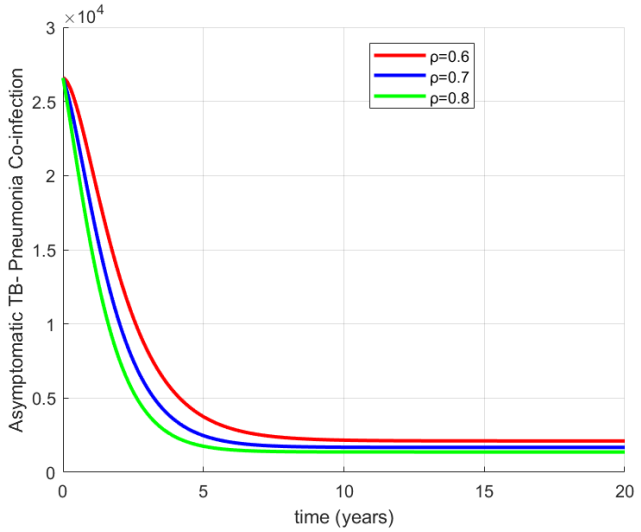

Figure 7. *Effects of varying vaccine efficacy* (ρ) *on asymptomatic tuberculosis-pneumonia co-infection.*

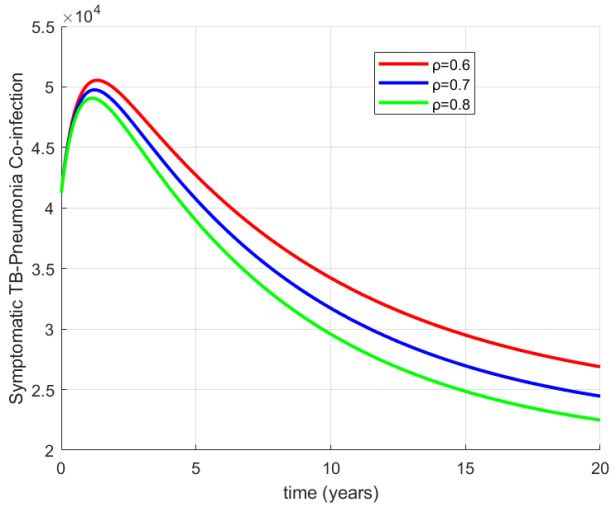

Figure 8. *Effects of varying vaccine efficacy* (ρ) *on symptomatic tuberculosis-pneumonia co-infection.*

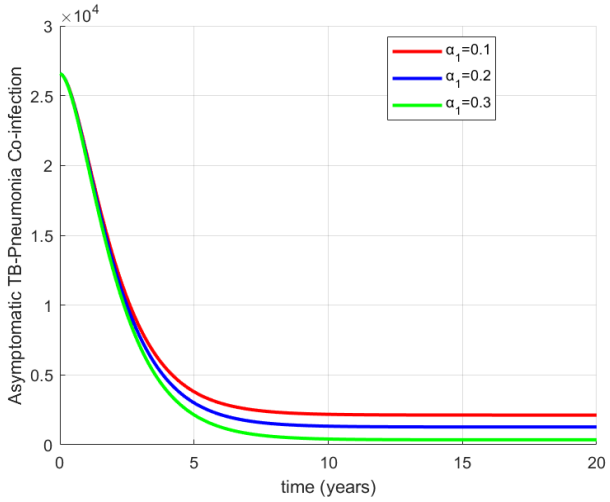

Figure 9. *Effects of varying the screening rate* (α_1) *for latently infected individuals on asymptomatic tuberculosis-pneumonia co-infection.*

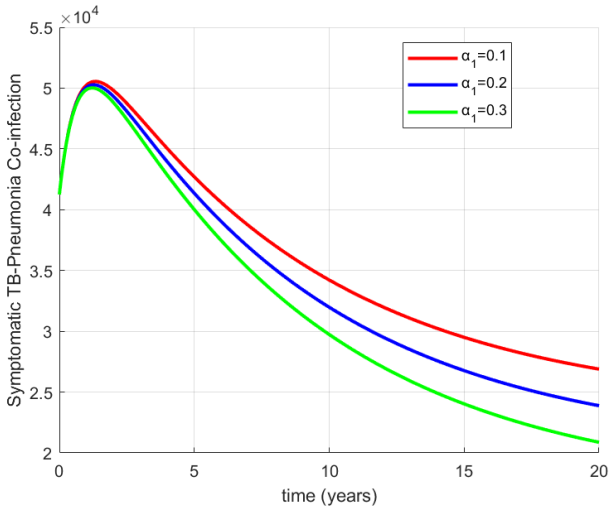

Figure 10. *Effects of varying the screening rate* (α_1) *for latently infected individuals on symptomatic tuberculosis-pneumonia co-infection.*

4.5. Effects of Varying Screening Rate for Latently Infected on Co-Infected Populations

In the flow chart depicted in Figure 1, α_1 represents the screening rate for latent tuberculosis infections. Figures 9 and 10 illustrate the effects of screening the latently infected population on tuberculosis-pneumonia co-infections. The results show that increasing the screening rate for latently infected individuals reduces tuberculosis-pneumonia co-infections. This reduction is attributed to a lower transmission rate of infections, resulting from decreased reactivation of latent infections. Consequently, this decline not only reduces the risk of infection transmission but also eases the burden on healthcare resources required for treating severe tuberculosis

cases, particularly in sub-Saharan African countries.

5. Conclusion

In this paper, a mathematical model of pulmonary tuberculosis in the presence of opportunistic pneumonia was formulated. The model integrates opportunistic pneumonia into the mathematical framework for pulmonary tuberculosis, based on clinical evidence of a lethal synergism between the two diseases. It accounts for the role of natural immunity in controlling or reducing infection transmission by incorporating a saturated progression from latent infection to active pulmonary tuberculosis using Holling's function. Additionally, the model includes the impact of screening asymptomatic tuberculosis patients on co-infections with pulmonary tuberculosis and opportunistic pneumonia. The inclusion of asymptomatic individuals is justified by a 2025 WHO report, which revealed that approximately 50% of people with pulmonary TB identified through global prevalence surveys are asymptomatic yet infectious.

Sensitivity analysis and numerical simulations were conducted to evaluate the effectiveness of various strategies for controlling co-infections. These strategies include enhancing natural immunity, screening asymptomatic and latently infected individuals, improving vaccine efficacy, and treating patients with severe tuberculosis. Sensitivity analysis revealed that reducing the transmission of pulmonary tuberculosis and improving vaccine efficacy are the most effective strategies for containing co-infections. Numerical simulations further indicate that increasing screening rates for asymptomatic and latently infected individuals reduces the number of co-infected cases. Additionally, increasing treatment rates for patients with severe tuberculosis and enhancing immunity among the latently infected also lead to a decline in co-infections.

Therefore, this study recommends greater emphasis on preventive measures against pulmonary tuberculosis and the improvement of vaccine efficacy to reduce the prevalence of pulmonary tuberculosis and pneumonia co-infection. It also recommends the screening of asymptomatic pulmonary tuberculosis patients and the enhancement of natural immunity among latently infected individuals to further reduce co-infections with pulmonary tuberculosis and opportunistic pneumonia.

The limitations of this study, which could be addressed in future research, include developing an optimal control and cost-effectiveness framework to identify the most effective intervention strategies at minimal cost; applying a stochastic approach to investigate the impact of randomness on the transmission dynamics of the diseases considered; utilizing a fractional-order model to enhance the accuracy of the results; and employing artificial intelligence techniques to identify asymptomatic infectious individuals within the population.

Abbreviations

TB	Tuberculosis
S	Susceptible
E	Exposed
I	Infectious
R	Recovered
N	Total Human Population

Author Contributions

Erick Mutwiri Kirimi: Conceptualization, Data curation, Formal Analysis, Investigation, Methodology, Project administration, Resources, Software, Validation, Visualization, Writing - original draft, Writing - review & editing

Jeconiah Okelo: Conceptualization, Data curation, Formal Analysis, Investigation, Methodology, Project administration, Resources, Software, Supervision, Validation, Visualization, Writing - original draft, Writing - review & editing

Mark Kimathi: Conceptualization, Data curation, Formal Analysis, Investigation, Methodology, Project administration, Resources, Software, Supervision, Validation, Visualization, Writing - original draft, Writing - review & editing

Kenneth Ngure: Conceptualization, Data curation, Formal Analysis, Investigation, Methodology, Project administration, Resources, Software, Supervision, Validation, Visualization, Writing - original draft, Writing - review & editing

Data Availability Statement

The data used to support the findings of this study is included in the article.

Funding

This research did not receive any specific grant from funding agencies in the public, commercial, or not-for-profit sectors.

Conflicts of Interest

The authors declare no conflicts of interest.

References

[1] World Health Organization. (2023). *Global tuberculosis report 2023*. Retrieved May 10, 2025, from https://www.who.int/publications/i/item/9789240083851

[2] National Tuberculosis, Leprosy and Lung Disease Program. *2023 Annual Report.* Ministry of Health, Kenya. Retrieved May 21, 2025, from https://nltp.co.ke/wp-content/uploads/2025/03/2023-Annual-Report.pdf

[3] Ullah, N., Fusco, L., Ametrano, L., Bartalucci, C., Giacobbe, D. R., Vena, A., & Bassetti, M. (2025). Diagnostic Approach to Pneumonia in Immunocompromised Hosts. *Journal of Clinical Medicine*, *14*(2), 389. https://doi.org/10.3390/jcm14020389

[4] Gweryina, R. I., Madubueze, C. E., Bajiya, V. P., & Esla, F. E. (2023). Modeling and analysis of tuberculosis and pneumonia co-infection dynamics with cost-effective strategies. *Results in Control and Optimization, 10*, 100210. https://doi.org/10.1016/j.rico.2023.100210

[5] Baguelin, M., Medley, G. F., Nightingale, E. S., O'Reilly, K. M., Rees, E. M., Waterlow, N. R., & Wagner, M. (2020). Tooling-up for infectious disease transmission modelling. *Epidemics, 32*, 100395. https://doi.org/10.1016/j.epidem.2020.100395

[6] Yan, P., & Chowell, G. (2019). *Quantitative methods for investigating infectious disease outbreaks* (Vol. 70). Cham, Switzerland: Springer. https://link.springer.com/book/10.1007/978-3-030-21923-9

[7] World Health Organization. (2023). *Tuberculosis fact sheet*. Retrieved May 14, 2025, from https://www.who.int/news-room/fact-sheets/detail/tuberculosis

[8] Chandra, P., Grigsby, S. J., & Philips, J. A. (2022). Immune evasion and provocation by Mycobacterium tuberculosis. *Nature Reviews Microbiology*, *20*(12), 750-766. https://www.nature.com/articles/s41579-022-00763-4

[9] Kirimi, E. M., Muthuri, G. G., Ngari, C. G., & Karanja, S. (2024). Modeling the effects of vaccine efficacy and rate of vaccination on the transmission of pulmonary tuberculosis. *Informatics in Medicine Unlocked*, *46*, 101470. https://doi.org/10.1016/j.imu.2024.101470

[10] Kirimi, E. M., Muthuri, G. G., Ngari, C. G., & Karanja, S. (2024). A Model for the Propagation and Control of Pulmonary Tuberculosis Disease in Kenya. *Discrete Dynamics in Nature and Society*, *2024*(1), 5883142. https://doi.org/10.1155/2024/5883142

[11] Li, Q., & Wang, F. (2023). An epidemiological model for tuberculosis considering environmental transmission and re-infection. *Mathematics*, *11*(11), 2423. https://doi.org/10.3390/math11112423

[12] Alfiniyah, C., Soetjianto, W. S. P. A., Aziz, M. H. N., & Ghadzi, S. M. B. S. (2024). Mathematical modeling and optimal control of tuberculosis spread among smokers with case detection. *AIMS Mathematics*, *9*(11), 30472-30492. https://www.aimspress.com/journal/Math

[13] Xu, C., Cheng, K., Guo, S., Yuan, D., & Zhao, X. (2024). A dynamic model to study the potential TB infections and assessment of control strategies in China. *arXiv preprint arXiv: 2401.12462*. https://doi.org/10.48550/arXiv.2401.12462

[14] Wang, J., & Lyu, G. (2024). Analysis of an age‐space structured tuberculosis model with treatment and relapse. *Studies in Applied Mathematics*, *153*(1), e12700. https://doi.org/10.1111/sapm.12700

[15] Oshinubi, K., Peter, O. J., Addai, E., Mwizerwa, E., Babasola, O., Nwabufo, I. V.,... & Agbaje, J. O. (2023). Mathematical modelling of tuberculosis outbreak in an East African country incorporating vaccination and treatment. *Computation*, *11*(7), 143. https://doi.org/10.3390/computation11070143

[16] Kasereka, S. K. (2024). Dynamics of a Tuberculosis Outbreak Model in a Multi-scale Environment. *arXiv preprint arXiv: 2411.04297*. https://doi.org/10.48550/arXiv.2411.04297

[17] Ochieng, F. O. (2025). Mathematical Modeling of Tuberculosis Transmission Dynamics With Reinfection and Optimal Control. *Engineering Reports*, *7*(1), e13068. https://doi.org/10.1002/eng2.13068

[18] Njeri, A. W., Kanyiri, C., & Okwanyi, I. (2024). Mathematical Analysis of Pneumonia Dynamics with Misdiagnosis. *Journal of African Interdisciplinary Studies*, *8*(8), 238-255.

[19] Chukwu, C. W., Tchoumi, S. Y., & Diagne, M. L. (2024). A simulation study to assess the epidemiological impact of pneumonia transmission dynamics in high-risk populations. *Decision Analytics Journal*, *10*, 100423. https://doi.org/10.1016/j.dajour.2024.100423

[20] Ndendya, J. Z., & Liana, Y. A. (2024). Mathematical Model and Analysis of Pneumonia on Children under five years with Malnutrition. *Available at SSRN 4692559*. https://dx.doi.org/10.2139/ssrn.4692559

[21] Mumbu, A. (2024). Modeling dynamics and stability analysis of pneumonia disease infection with parameters uncertainties control. *Mathematics Open*, *3*, 2430001. https://doi.org/10.1142/S2811007224300015

[22] Aldila, D., Awdinda, N., Herdicho, F. F., Ndii, M. Z., & Chukwu, C. W. (2023). Optimal control of pneumonia transmission model with seasonal factor: learning from Jakarta incidence data. *Heliyon*, *9*(7). https://doi.org/10.1016/j.heliyon.2023.e18096

[23] Tilahun, G. T., Makinde, O. D., & Malonza, D. (2017). Modelling and optimal control of pneumonia disease with cost-effective strategies. *Journal of biological dynamics*, *11*(sup2), 400-426. https://doi.org/10.1080/17513758.2017.1337245

[24] Olopade, I. A., Akinola, E. I., Philemon, M. E., Mohammed, I. T., Ajao, S. O., Sangoniyi, S. O., & Adeniran, G. A. (2024). Modeling the mathematical transmission of a pneumonia epidemic model with awareness. *Journal of Applied Sciences and Environmental Management*, *28*(2), 403-413. https://doi.org/10.4314/jasem.v28i2.11

[25] Shrestha, S., & Shrestha, A. (2024). Mathematical modelling to accurately quantify the benefits of pneumococcal conjugate vaccine. *The Lancet Global Health*, *12*(9), e1377-e1378. https://www.thelancet.com/action/showPdf?pii=S2214-109X%2824%2900323-1

[26] Yano, T. K., & Bitok, J. (2022). Computational Modelling of Pneumonia Disease Transmission Dynamics with Optimal Control Analysis. *Appl. Comput. Math*, *11*(5), 130-139. https://doi.org/10.11648/j.acm.20221105.13

[27] World Health Organization. (2025). *Report of the WHO consultation on asymptomatic tuberculosis, Geneva, Switzerland, 14-15 October 2024*. Retrieved May 4, 2025, from https://iris.who.int/bitstream/handle/10665/380616/9789240106932-eng.pdf

[28] World Health Organization. (2025). *Integrated approach to tuberculosis and lung health: Policy brief*. Geneva: World Health Organization. Licence: CC BY-NC-SA 3.0 IGO. Retrieved May 14, 2025, from https://iris.who.int/bitstream/handle/10665/380840/9789240107526-eng.pdf%20?sequence=1

[29] Banerjee, S. (2021). *Mathematical modeling: models, analysis and applications*. Chapman and Hall/CRC. https://doi.org/10.1201/9781351022941

[30] Kizito, M., Nampala, H., & Ariho, P. (2024). Mathematical Modelling of Tuberculosis and Hepatitis C Coinfection Dynamics with No Intervention. *Journal of Mathematics*, *2024*(1), 5521979. https://doi.org/10.1155/2024/5521979

[31] Khajanchi, S., Das, D. K., & Kar, T. K. (2018). Dynamics of tuberculosis transmission with exogenous reinfections and endogenous reactivation. *Physica A: Statistical Mechanics and its Applications*, *497*, 52-71. https://doi.org/10.1016/j.physa.2018.01.014

[32] Driessche, K., Khajanchi, S., & Kar, T. K. (2020). Transmission dynamics of tuberculosis with multiple re-infections. *Chaos, Solitons & Fractals*, *130*, 109450. https://doi.org/10.1016/j.chaos.2019.109450

[33] La Salle, J. P. (1976). *The stability of dynamical systems*. Society for Industrial and Applied Mathematics. https://doi.org/10.1137/1.9781611970432

[34] Khajanchi, S., Bera, S., & Roy, T. K. (2021). Mathematical analysis of the global dynamics of a HTLV-I infection model, considering the role of cytotoxic T-lymphocytes. *Mathematics and Computers in Simulation*, *180*, 354-378. https://doi.org/10.1016/j.matcom.2020.09.009

[35] Chowell, G., & Kiskowski, M. (2016). Modeling ring-vaccination strategies to control Ebola virus disease epidemics. *Mathematical and statistical modeling for emerging and re-emerging infectious diseases*, 71-87. https://doi.org/10.1007/978-3-319-40413-4

[36] KNBS 2023. *Statistical Abstract 2023*. Nairobi, Kenya. Retrieved May 21, 2025, from https://www.knbs.or.ke/wp-content/uploads/2023/11/2023-Statistical-Abstract.pdf

[37] National Tuberculosis, Leprosy and Lung Disease Program. *National strategic plan for tuberculosis, leprosy and lung health 2019-2023.* Ministry of Health, Kenya. Retrieved May 23, 2025, from https://nltp.co.ke/reports/annual-reports/

[38] National Tuberculosis, Leprosy and Lung Disease Program. *2021 Annual Report.* Ministry of Health, Kenya. Retrieved May 26, 2025, from https://nltp.co.ke/reports/annual-reports/

[39] National Tuberculosis, Leprosy and Lung Disease Program. *Kenya latent tuberculosis infection policy 2020*. Ministry of health, Kenya. Retrieved May 21, 2025, from https://nltp.co.ke/reports/annual-reports/

[40] National Tuberculosis, Leprosy and Lung Disease Program. *2022 Annual Report.* Ministry of Health, Kenya. Retrieved May 21, 2025, from https://nltp.co.ke/reports/annual-reports/